

Project: Nanoscale Architectural Engineering for High-Performance Solid Oxide Fuel Cells

Stanford subaward agreement number: 18943600-38962-A

Final Report (Public Version)
Reporting period: 08-03-2007 to 04-30-2010

Submitted to: Dr. Sallie Benson and Dr. Richard Sassoon

Submitted by: Sossina M. Haile
California Institute of Technology, Materials Science, 309-81
Pasadena, CA 91125
Phone: 626-395-2985; Email: smhaile@caltech.edu

Participants: Prof. David G. Goodwin (co-principle investigator), Dr. David A. Boyd (research associate), Dr. Marion R. Martin (post-doctoral scholar, fellowship-supported), Dr. Yong Hao (post-doctoral scholar), Eugene Mahmoud (graduate student), William C. Chueh (graduate student, partial fellowship-support), Evan C. Brown (graduate student), Taesik Oh (graduate student, fellowship-supported), Stephen Wilke (undergrad student), Changyi Li (undergraduate student), Joy Sheng (undergraduate student, fellowship-supported)

Abstract

The lofty goal of this program is to combine advanced materials with advanced nano- and micro-scale fabrication methods to build SOFC structures with unparalleled performance (power output of 10 W/cm^2 at $600 \text{ }^\circ\text{C}$) at reasonable cost. Key to this effort is a fundamental understanding of the structure-properties relationships governing global electrochemical reaction rates at fuel cell electrodes. We have established that, in addition to the conventional triple-phase boundaries (oxide-metal-gas) the two-phase boundaries (oxide-gas) boundaries in ceria-electrolyte fuel cells are high activity for hydrogen electro-oxidation. For oxygen electro-reduction, we find that a reversible, bulk phase transformation between cubic and hexagonal phases has a dramatic impact on interfacial impedance, despite the reaction being surface limited. Our fabrication efforts encompass pulsed laser deposition (PLD) of both dense and porous ceria, conformal film deposition by chemical vapor deposition (CVD), electrochemical deposition of porous ceria, electrochemical infiltration of nano-porous anodic aluminum oxide (AAO) with ceria as a route to nanowires, and preparation of patterned, thermally stable 2-D metal electrodes by both conventional photolithography and self-assembled polymer sphere lithography. The combination of synthetic tools and firm quantification attained here uniquely positions us to achieve the goal of ultra-high power density solid oxide fuel cells.

Introduction

The lofty goal of this program is to combine advanced materials with advanced nano- and micro-scale fabrication methods to build SOFC structures with unparalleled performance at reasonable cost. To this end, we have proposed a fuel cell that utilizes doped ceria as the electrolyte, the advanced perovskite BSCF ($\text{Ba}_{0.5}\text{Sr}_{0.5}\text{Co}_{0.8}\text{Fe}_{0.2}\text{O}_{3-\delta}$)¹ as the cathode and a metal-ceria framework as the anode. Our simulations suggest that peak power densities of 10 W/cm^2 are possible for such fuel cells operated on hydrogen at $600 \text{ }^\circ\text{C}$ when care is taken to optimally construct and integrate the SOFC components. The construction requirements include preparation of (1) thin ($2\text{-}3 \mu\text{m}$) electrolytes that are free of grain boundary resistance effects, (2) hierarchically structured electrodes with micrometer-scale pores for gas flow and nanometer-scale wires or particles for catalysis, and (3) electrodes with highly interconnected networks of ion conductor, electron conductor, and pores. Our efforts have spanned these fabrication objectives as well as advancing our fundamental understanding of the structure-property relationships in SOFC electrodes.

Background

The highest power output reported to date for SOFC operation at $600 \text{ }^\circ\text{C}$, 1.95 W/cm^2 , remains that reported by Ishihara and coworkers² in 2006 (where humidified hydrogen served as the fuel and neat oxygen as the oxidant). The fuel cell components were SSC (presumably $\text{Sr}_{0.5}\text{Sm}_{0.5}\text{CoO}_{3-\delta}$, though not explicitly stated) as the cathode, LSGM ($\text{La}_{0.9}\text{Sr}_{0.1}\text{Ga}_{0.8}\text{Mg}_{0.2}\text{O}_3$) as the electrolyte, a mixture of the metal alloy Ni(80)-Fe(20) and the ceramic SDC (samaria doped ceria, or $\text{Ce}_{0.8}\text{Sm}_{0.2}\text{O}_{2-\delta}$) as the anode, and SDC as a buffer layer between the electrolyte and the anode. Thin electrolyte ($\sim 5 \mu\text{m}$) and buffer ($\sim 400 \text{ nm}$) layers were obtained by pulse-layer deposition onto dense, anode precursor substrates formed of NiO- Fe_3O_4 -SDC. The substrates were subsequently reduced to convert the metal oxides to the metal and generate porosity in the anodes. The cathode was deposited by slurry-coating. The thickness of neither electrode was reported.

The Ishihara result demonstrates quite clearly that high power densities are indeed achievable using advanced materials and modern fabrication tools. In contrast to the proposed work, these authors have not taken advantage of a full understanding of electrochemical reaction pathways to design electrode structures that can advance power outputs even further. Moreover, the materials selected do not represent the highest performance possibilities. Specifically, BSCF has higher activity for oxygen electroreduction than SSC, and SDC has higher ionic conductivity than LSGM (and at $600 \text{ }^\circ\text{C}$ and lower, the electronic conductivity of SDC has negligible detrimental impact on fuel cell voltage). These characteristics are reflected in the fact that after the Ishihara result, the next highest performing fuel cells at $600 \text{ }^\circ\text{C}$ incorporate doped ceria electrolytes and BSCF cathodes. These include the cell³ BSCF | $10 \mu\text{m}$ GDC | GDC-Ni (where GDC = gadolinia doped ceria), with a peak power density of 1.33 W/cm^2 , and the cell¹ BSCF | $20 \mu\text{m}$ SDC | SDC-Ni, with a peak power density of 1.01 W/cm^2 .

Based on these successes we proposed that ultra-high power density would be attainable by combining these modern materials with validated design principles and modern fabrication routes. We report here advances in both the fundamental science that places the design approach on a firm understanding of electrochemical reaction pathways and the actual construction of high surface area electrodes.

Results

Fundamental Electrochemistry: Hydrogen electro-oxidation. The overall strategy proposed here is differentiated from approaches pursued in the literature in that we recognize that ceria, nominally an electrolyte material, becomes sufficiently electronically conducting under the reducing conditions of a fuel cell anode such that its inherent catalytic activity plays a direct role in the electrochemical reactions. While much circumstantial evidence from our lab and others supported this view prior to the initiation of this GCEP project, direct evidence was lacking. Under GCEP support we have characterized the activity of doped ceria directly at the gas-oxide two-phase boundary, *i.e.* in the absence of triple phase boundaries that would otherwise convolute the data. As shown in Figure 1 this is achieved by embedding metal (typically Pt) current-collectors beneath a dense film of doped ceria, deposited by pulsed laser deposition (PLD) atop yttria stabilized zirconia (a pure ionic conductor). The electronic conductivity is sufficiently high that electronic charge carrier transport to the surface from the current collectors (or vice versa) can keep pace with any surface electrochemistry. As there is no gas-phase access to the metal, any detected electrochemistry must be that which occurs on the two-phase boundary between the ceria and the gas-phase. From these measurements, we obtain an interfacial area specific resistivity of $25 \Omega\text{cm}^2$ at $600 \text{ }^\circ\text{C}$, $p_{\text{H}_2} = 0.49 \text{ atm}$, and $p_{\text{H}_2\text{O}} = 0.022 \text{ atm}$, typical SOFC anode conditions.

To establish the triple-phase boundary (TPB) activity, we performed a series of experiments in which Ni strips were patterned onto the surface of SDC (a somewhat more conventional arrangement). The exposed surface area of SDC was fixed whereas the TPB density was varied by varying the pattern repeat distance, Figure 2. For electrochemically active TPBs, the area specific interfacial resistance depends inversely on the specific TPB length. Hence, from the slope of $1/\rho_{\text{int}}$ vs. specific TPB length, we measure the length specific interfacial resistance at the Ni-SDC-gas interface to be $4.2 \times 10^4 \Omega\text{cm}$. The intercept of $1/\rho_{\text{int}}$ vs. specific TPB length provides a second, independent measure of the interfacial resistance at the ceria-gas interface. The value of $26 \Omega\text{cm}^2$ obtained from this extrapolation technique is in good agreement with the value obtained from the direct measurement described above.

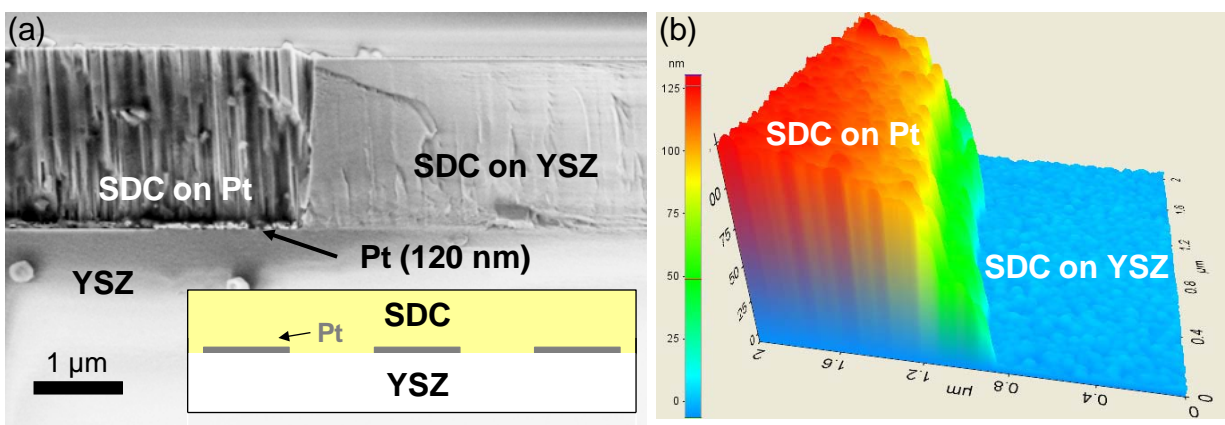


Figure 1. Pt electrode embedded under a dense film of SDC (samarium doped ceria) for the direct measurement of the SDC-gas interfacial reaction resistance for hydrogen electro-oxidation: (a) cross-sectional SEM image with inset showing schematic structure, and (b) AFM image showing surface topology.

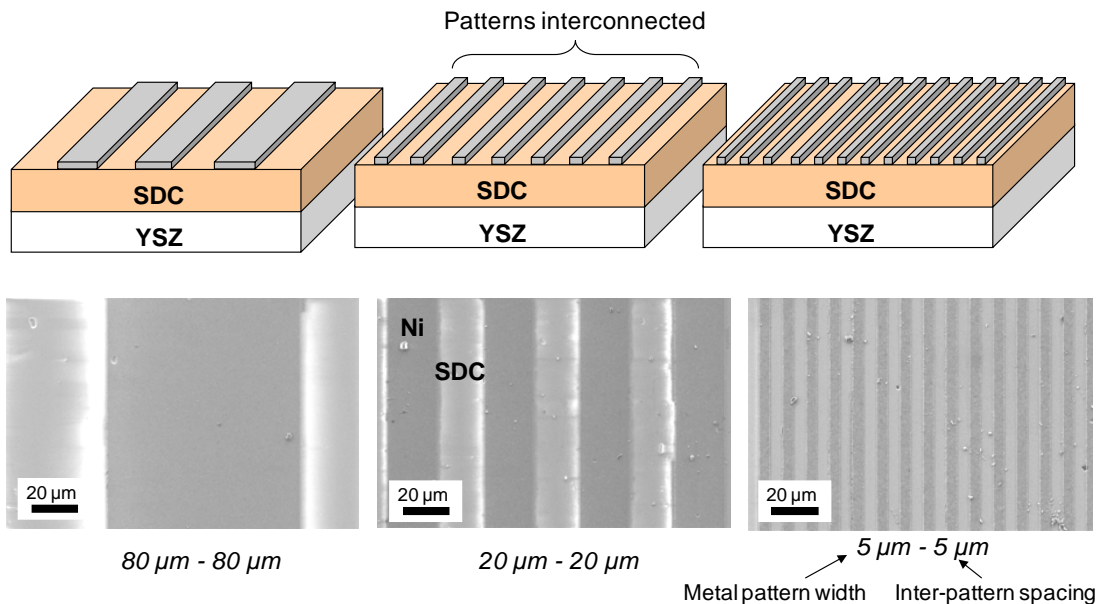


Figure 2. Schematic and SEM plan-view of patterned metal electrodes on SDC (samarium doped ceria), in turn, deposited on single crystal YSZ (yttria-stabilized zirconia). Total triple-phase boundary (TPB) length increases as the pattern dimensions are decreased (to the right), but the exposed SDC surface area is constant throughout.

Fundamental Electrochemistry: Oxygen electro-reduction. The high activity of $\text{Ba}_{0.5}\text{Sr}_{0.5}\text{Co}_{0.8}\text{Fe}_{0.2}\text{O}_{3-\delta}$ (BSCF) as a solid oxide fuel cell cathode was reported by the Haile group in 2004.¹ In our early measurements we established that the material crystallizes as an ideal cubic perovskite, has an exceptionally high concentration of oxygen vacancies ($\delta \sim 0.5$), and an exceptionally high oxygen diffusion rate. We also found that the electrochemical reduction of oxygen for typical cathode configurations was surface reaction limited, rather than bulk diffusion transport limited. The electronic transference number is high, close to 1, and as such electron transport is high, and is not rate-limiting for sufficiently short distances (less than about $10 \mu\text{m}$). For porous cathodes deposited onto dense SDC, the interfacial reaction resistance at $600 \text{ }^\circ\text{C}$ was found to be $\sim 0.07 \Omega\text{cm}^2$. Under GCEP support we have begun to unravel the surface reaction behavior of BSCF through the use of dense, thin-film cathodes grown by pulsed laser deposition. After an exhaustive examination of the parameter space for film deposition, we have identified growth conditions that ensure sufficient fidelity between the stoichiometry of the source (or target) material and that of the film. Impedance characterization using the embedded electrode geometry indicates the activity of the BSCF surface to be $\sim 1.3 \Omega\text{cm}^2$ (interfacial area-specific reaction resistance), a factor of twenty more resistive than the randomly porous analog. The result emphasizes the role of electrode surface area for lowering cell impedance. Our measurements also suggest that BSCF can undergo a reversible phase transformation at temperatures between ~ 550 and $700 \text{ }^\circ\text{C}$ from the desirable cubic phase to a less active, probably hexagonal phase. Prolonged measurements at these temperatures reveal a slow increase in interfacial reaction resistance over time. A short anneal at $875 \text{ }^\circ\text{C}$ restores the high electrochemical activity, indicating that the process does not involve volatilization or any other irreversible changes to the material. It is this observation, along with direct diffraction data, that lead us to conclude that the loss in activity is associated with a transformation to a hexagonal phase.

Fabrication of 2-D Metal Electrodes. Our ability to perform quantitative electrochemical studies depends in large part on our ability to prepare patterned electrodes with controlled and thermally stable features, at relevant dimensions (microns to submicron). Linear patterns of a broad spectrum of metals (Pt, Ni, Cu, Ag, Au) have been obtained by photolithography, which allows access to pattern dimensions between several and tens of micrometers. Extensive study of the coarsening and dewetting behavior of these films at high temperatures indicates that film thickness is the key parameter controlling morphological stability. Sufficiently thick films can be annealed at temperatures as high as $\sim 70\%$ of the melt temperature for many hours without significant dimensional changes. Examples of Ni and Cu patterned strip electrodes with excellent thermal stability under hydrogen are presented in Figure 3.

While electrodes of the type presented above have proven extremely beneficial for quantitative electrochemical studies, the minimum feature size attainable by conventional photolithography, $\sim 5 \mu\text{m}$, limits the range of accessible electrochemical measurements and provides insufficient triple phase boundary density for fuel cell preparation. To obtain smaller feature sizes, we have pursued a facile sacrificial templating method, known as polymer sphere lithography, to deposit a fully connected, yet fully porous ‘anti-dot’ metallic thin-film⁴ on fuel cell electrolyte materials. In brief, an ordered monolayer of monodisperse polystyrene beads is applied to the surface of the substrate, the beads are etched in an oxygen plasma to create vias between them, a line-of-site thermal evaporation step is used to deposit a thin-layer of the metal of choice, and, finally, the beads are removed, Figure 4. Using this method, porous metal films of nickel, gold/titanium, copper, and aluminum have been deposited on yttria-stabilized zirconia (YSZ) and samaria-doped ceria (SDC) single crystals. Starting beads of diameters $0.5 - 3.2 \mu\text{m}$ are used, yielding pore and interpore feature sizes of $0.3 - 2.5 \mu\text{m}$, Figure 5.

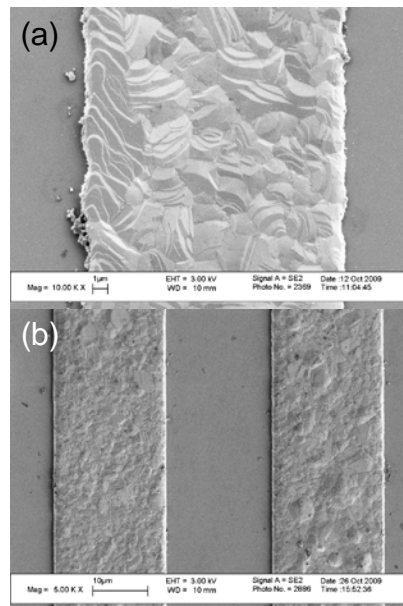


Figure 3. Thermally stable thin-film metal patterns: (a) $20\mu\text{m}$ -metal- $20\mu\text{m}$ -space Ni pattern ($0.6 \mu\text{m}$ thickness) treated at 900°C in $20\% \text{H}_2$ for 24 h; (b) $20\mu\text{m}$ -metal- $20\mu\text{m}$ -space Cu pattern treated at 700°C in $20\% \text{H}_2$ for 24 h.

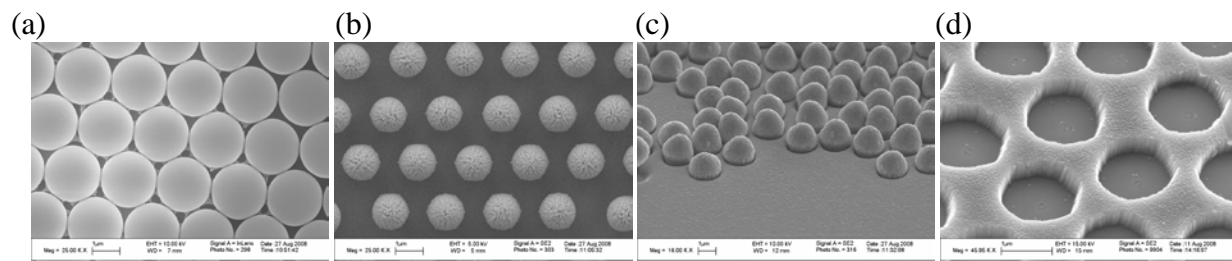


Figure 4. Sacrificial templating process: (a) polystyrene (PS) bead monolayer on single crystal YSZ (yttria stabilized zirconia), (b) diameter reduced via oxygen plasma etching, (c) metal (Cu) deposited by thermal evaporation, (d) PS beads removed.

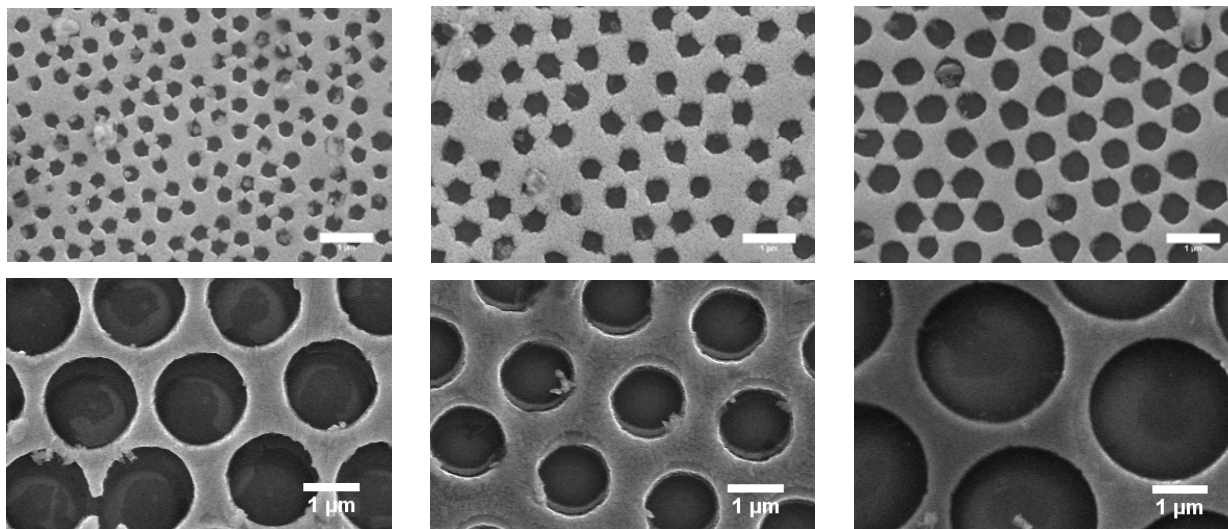


Figure 5. Highly tunable, wide-ranging feature sizes developed by the polymer sphere lithography technique. Scale bar in all images is 1 μm .

Fabrication of Ceria Films: Dense Electrolytes and Porous Electrodes. A broad range of fabrication tools have been developed for the preparation of ceria-based components of SOFCs – dense, thin-film electrolyte or high surface area, high porosity electrodes. We have had particular success with pulsed laser deposition (PLD) of 15% Sm-doped ceria (SDC15). Simply by varying the oxygen partial pressure during deposition, we can deposit either epitaxial thin films (50 mTorr $p\text{O}_2$) or columnar porous films (100 mTorr $p\text{O}_2$), Figure 6. Electrochemical impedance characterization of the porous thin film in hydrogen atmosphere showed a 24 \times improvement in the surface reaction rate over the dense film, underscoring the role of surface area in establishing fuel cell performance. The films furthermore display excellent thermal stability against microstructural evolution at 900 $^\circ\text{C}$ (24 h exposure).

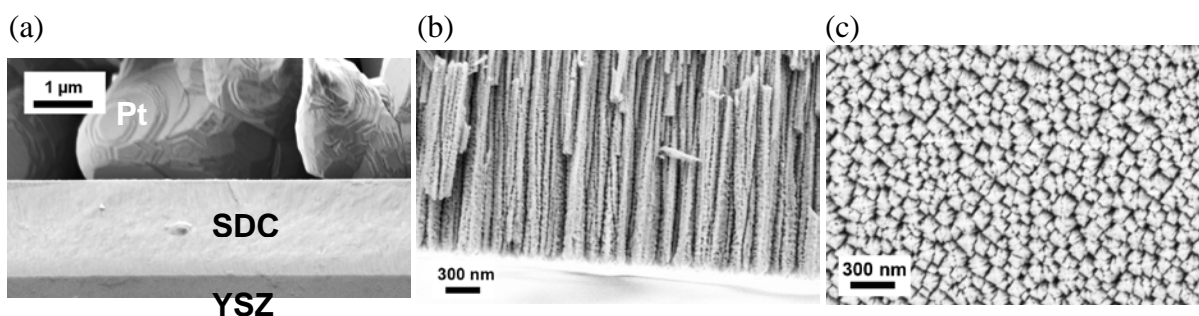


Figure 5. Cross-section scanning electron micrographs of (a) dense ceria thin film and (b) porous columnar ceria thin film deposited by PLD (with the planer view shown in (c)).

Summary

Over the course of this three year program, we have developed a vast and powerful array of fabrication tools for the preparation of ultra-high power density solid oxide fuel cells. We have further attained highly quantitative electrochemical data that allow us one on the one hand to begin to elucidate reaction pathways and on the other hand to provide rational design of high performance electrodes. This combination of synthetic tools and firm quantification uniquely positions us to revolutionize the science and technology of solid oxide fuel cells. The successes

we have demonstrated to date put us well along the path to solid oxide fuel cells with 10 W/cm² power outputs. Such high power outputs imply exceptionally high chemical to electrical energy conversion efficiencies and thereby dramatic reductions in chemical energy consumption and CO₂ emissions.

Publications

1. E. C. Brown, S. K. Wilke, D. A. Boyd, D. G. Goodwin and S. M. Haile, "Polymer Sphere Lithography for Solid Oxide Fuel Cells: A Route to Functional, Well-Defined Electrode Structures" *J. Mat. Chem.* **20**, 2190-2196 (2010).
2. W. C. Chueh and S. M. Haile, "Electrochemical Studies of Capacitance in Cerium Oxide Thin Films and Its Relationship to Anionic and Electronic Defect Densities," *Phys. Chem. Chem. Phys.* **11**, 8144 - 8148 (2009).

Literature References

1. Shao, Z. P.; Haile, S. M., A high-performance cathode for the next generation of solid-oxide fuel cells. *Nature* **2004**, 431, (7005), 170-173.
2. Ishihara, T.; Yan, J. W.; Shinagawa, M.; Matsumoto, H., Ni-Fe bimetallic anode as an active anode for intermediate temperature SOFC using LaGaO₃ based electrolyte film. *Electrochimica Acta* **2006**, 52, (4), 1645-1650.
3. Liu, Q. L.; Khor, K. A.; Chan, S. H., High-performance low-temperature solid oxide fuel cell with novel BSCF cathode. *Journal of Power Sources* **2006**, 161, (1), 123-128.
4. E. Spada, A. Da Rocha, E. Jasinski, G. Pereira, L. Chavero, A. Oliveira, A. Azevedo and M. Sartorelli, *J. Appl. Phys.*, **2008**, 103, 114306-5.